nature nanotechnology

SUPPLEMENTARY INFORMATION

DOI: 10.1038/NNANO.2015.295

Spin-torque resonant expulsion of the vortex core for an efficient radiofrequency detection scheme

DOI: 10.1038/NNANO.2015.295

Frequency dependence of the excitation radius

The projection of the Thiele equation applied to the vortex in the radial u_ρ and orthoradial u_θ axes can be expressed as the following [1]

$$G\rho\dot{\theta} - D\dot{\rho} - \kappa_{ms}\rho = 0 \qquad (u_\rho), \tag{1}$$

$$-D\rho\dot{\theta} - G\dot{\rho} = 0 \qquad (u_\theta) \tag{2}$$

where G is the gyrovector, D is the damping term, D = $2\alpha\eta\pi LM_S/\gamma$, where α is the Gilbert damping and η is the damping constant and κ_{ms} is the magnetostatic vortex stiffness. This can be rewritten including the additional forces due to an applied polarised current, which are

$$F_{Slon\parallel} = -\pi\sigma_x CbM_S LJ\mathbf{u}_x = -\pi\sigma_x bJp_x M_S LCln2(cos\chi\mathbf{u}_\rho - sin\chi\mathbf{u}_\theta), \tag{3}$$

$$F_{Slon\perp} = \pi\sigma_z M_S LJ\rho\mathbf{u}_\theta, \tag{4}$$

$$F_{FLT} = \frac{2}{3}\pi\sigma_x CM_S LR\xi_{FLT}J\mathbf{u}_y = \frac{2}{3}C\pi M_S LRJ\xi_{FLT}\sigma_x(sin\chi\mathbf{u}_\rho + cos\chi\mathbf{u}_\theta), \tag{5}$$

$$F_{Oe} = -0.85C\mu_0 M_S LRJ\rho\mathbf{u}_\rho \tag{6}$$

where ρ is the vortex core shift with respect to the disk center, χ is the angle between $\mathbf{u}_x$ and the vortex core position. The vortex chirality and core size are given by C and b, respectively, and the thin film saturation magnetisation, thickness and radius are given by M_S, L and R. The spin transfer torque efficiency is given by $\sigma = \hbar P/2|e|LM_S$, where P is the polarisation which, as shown schematically in Fig. 1 a) in the main paper, has two components, p_x and p_z, which will vary as a function of the applied perpendicular magnetic field, H_{perp}. The relative efficiency of the field-like torque, ξ_{FLT}, is only relevant in magnetic tunnel junctions and has been previously reported at ξ_{FLT} = 0.4 [2] for strongly asymmetric tunnel junctions, similar to those reported here.

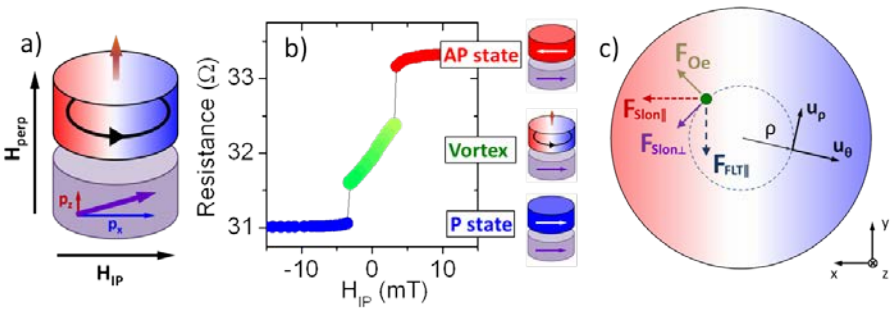

FIG. 1. **Magnetic vortices in magnetic tunnel junctions**. a) Schematic of the free layer, in the vortex configuration, and the top layer of the SAF, with polarisation components p_x and p_z and b) the in-plane magnetic field dependence of the resistance showing the parallel (P), vortex and antiparallel (AP) states. c) Top view of the current induced forces acting on the vortex core (green dot) due to the Oersted field, F_{Oe}, the Slonczewski torque due to an in-plane and perpendicularly polarised current, $F_{Slon\parallel}$ and $F_{Slon\perp}$, and the force due to the field-like torque for an in-plane polarised current, $F_{FLT\parallel}$.

The force due to the field-like torque associated with a perpendicularly polarised spin current will not actively contribute to the dynamics of the vortex core, but can result in a deformation of the core itself. The Oersted field will predominantly be important

in changing the natural frequency of the vortex by adjusting the potential felt by the core via the confinement, although if the chirality is aligned opposite to that of the current induced Oersted field, a sufficiently large d.c. current can result in chirality switching [3].

The Thiele equation, taking into account the spin polarised current, can therefore be rewritten as

$$G\rho\dot{\theta} - D\dot{\rho} - \kappa(I)\rho + J\Lambda_{Slon\parallel}cos\chi + J\Lambda_{FLT}sin\chi = 0 \qquad (u_\rho), \tag{7}$$

$$-D\rho\dot{\theta} - G\dot{\rho} + a_J J\rho - J\Lambda_{Slon\parallel}sin\chi + J\Lambda_{FLT}cos\chi = 0 \qquad (u_\theta) \tag{8}$$

where $\Lambda_{Slon} = -\pi\sigma_x CbM_S L$ and $\Lambda_{FLT} = \frac{2}{3}\pi\sigma_x CM_S LR\xi_{FLT}$, $a_J = \pi M_S Lp_z\sigma$ and $\kappa(I) = \kappa_{ms} + J\kappa_{Oe}$ where $\kappa_{Oe} = 0.85C\mu_0 M_S LR$.

For a time varying current, I(t) = I_{dc}+I_{rf} $\cos(\omega_S t)$, a resonant excitation of the vortex core can occur and will depend upon the phase of the incoming signal and the vortex core. In this respect, the resonant excitation is closely analogous to the injection locking of a vortex core in the steady state to an external current [4, 5]. The force associated with the Slonczewski torque polarised out-of-plane, $F_{Slon\perp}$, and the force due to the Oersted field, F_{Oe}, are independent of the phase, and for a continuous current will average to zero over a full period. The in-plane forces, $F_{Slon\parallel}$ and $F_{FLT\parallel}$, will not average to zero and are instead responsible for the resonant excitations of the vortex core via an rf current.

If the applied current is defined as J = J_{dc}+J_{rf}cos(ωt), $\omega = \dot{\theta}$ and $\chi = \omega t + \chi_0$, and we assume that $D^2 \ll G^2$, then the system can be solved for the first order (with the second order averaging to zero over a full period) at equilibrium, i.e. $\dot{\rho}$ = 0, for the orbit radius

$$\rho_{osc} = \frac{J_{rf}\sqrt{\Lambda_{Slon}^2 + \Lambda_{FLT}^2}}{2G\sqrt{\left(\omega - \frac{\kappa(J_{dc})}{G}\right)^2 + \frac{(-\pi\sigma p_z M_S LJ_{dc} + D\omega)^2}{G^2}}}. \tag{9}$$

Estimation of the radius from voltage peak

In Fig. 2 a), the excitation radius is estimated using Ohms law. The ratio of the oscillation magnetisation can be expressed in terms of the excitation radius [6]

$$\frac{\Delta M_{osc}}{M_S} = \lambda s_0, \tag{10}$$

where ΔM_{osc} is the time varying component of the magnetisation, M_S is the saturation magnetisation and that λ = 2/3 for an oscillation amplitude, ρ less than 60% of the total radius R, and $s_0 = \rho/R$.

The conductance can be described with a constant component, G_0, and a time varying component, ΔG_{osc}, such that

$$G = G_0 + \frac{\Delta G_{osc}}{2}\lambda s_0. \tag{11}$$

The resistance, 1/G, can be expressed as

$$R \simeq \frac{1}{G_0} + \frac{G_P - G_{AP}}{2G_0^2}\lambda s_0. \tag{12}$$

DOI: 10.1038/NNANO.2015.295

where $R_0 = 1/G_0$ is the resistance of the system when the core is stationary, G_P (G_{AP}) is the conductance in the parallel (antiparallel) state. The orbit radius, ρ_{osc}, can therefore be estimated as

$$\rho_{osc} \simeq \frac{2\Delta R_{osc}}{\lambda} \frac{2G_0^2}{G_P - G_{AP}} R. \tag{13}$$

where $\Delta R_{osc} = \sqrt{2V_{peak}/\Delta I_{rf}}$

Modelling the core expulsion with in-plane magnetic field

In figure 3. in the main paper, the core expulsion is present for two different in-plane magnetic fields, showing that the free layer magnetisation becomes parallel or anti-parallel relative to the polariser depending upon the sign of the in-plane field component. The expulsion of the vortex core can be modelled by assuming that the position of the core is described by $\rho = \rho_{osc} + \rho_{disp} + \rho_H$, where ρ_{osc} is the excitation radius due to the rf current found with Eq. 1, $\rho_{disp} = \sqrt{\left(\frac{J_{dc}}{2G\omega_0}\right)^2 (\Lambda_{SL}^2 + \Lambda_{FLT}^2)}$ is the displacement due to the dc current and comes from the solution of the Thiele equation at equilibrium, and ρ_H is the displacement of the vortex core from the centre of the junction due to H_{IP}.

As has been discussed previously, the field-like torque will produce a static shift of the vortex core equivalent to the application of an in-plane magnetic field. This means that when H_{IP} is applied in conjunction with a constant d.c. current, I_{dc} = 5 mA, the resultant core shift, in the absence of an rf current, will be $\rho = \rho_{disp} + \rho_H$, as the d.c. current effectively causes an offset in the magnetic field. This is demonstrated in Fig. 2, where the normalised excitation radius ρ/R is shown for two in-plane magnetic fields. The displacement of the vortex core due to the d.c. current is not equivalent for the two in-plane fields as in one case the field is acting with the d.c. current induced vortex shift (H_{IP} = 3 mT) and in the other case it is acting against the current induced shift (H_{IP} = -3 mT). When the static position of the vortex core is closer to the edge of the disk, a smaller rf induced excitation radius will result in the expulsion of the vortex core, which can be seen by the larger frequency range of expulsion (defined as $\rho > 0.75$R) demonstrated by the red and blue shaded areas in Fig. 2.

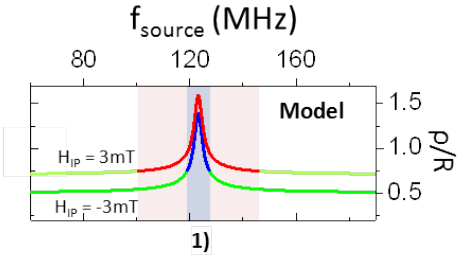

FIG. 2. The modelled normalised radius as a function of the excitation frequency for two in-plane fields, ±3 mT, showing that the core is expelled ($\rho > 0.75$R), for a different frequency range depending upon the sign of the field.

The removal of the vortex core from the free layer, and the resultant large change in resistance, can give rise to a maximum resistive change of $\sim \frac{1}{2}\Delta$R, where ΔR = R_{AP} - R_P and can be seen to be highly scalable with increasing TMR. Furthermore, this ability for the system to change from the vortex state to either the parallel or antiparallel state gives rise to the prospect of a 3 state memory, where the final state is determined by this very small in-plane field, $\sim$ 3 mT, the writing process of which may be controlled by a combination of rf and dc injected currents.

The core expulsion bandwidth

The bandwidth of the core expulsion is a crucial factor for potential applications, and for the case of the expulsion of the vortex core, the bandwidth is simply defined as the width of the resistance plateau. As seen in Fig. 3, the bandwidth increases linearly as a function of I_{rf}, meaning that the system shows a highly tunable and controllable bandwidth which can be tailored depending upon the specific needs of the potential application. The minimum bandwidth observed is around 1 MHz, which is highly competitive when compared to potential spin-diode based detectors, and certainly adequate to meet the needs of certain types of potential rf applications.

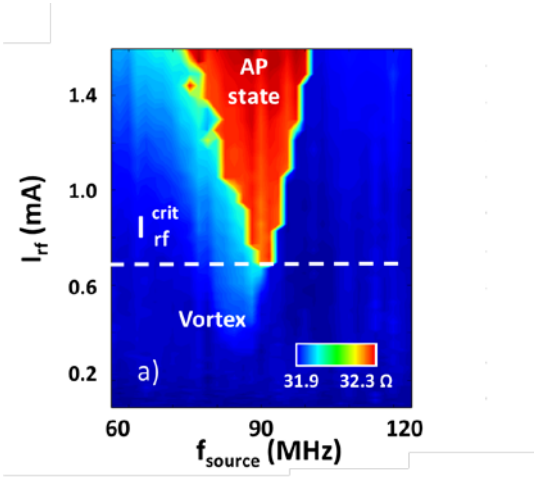

FIG. 3. Bandwidth of the expulsion as a function of the rf current, where the red region shows the AP state, where the core has been expelled.

[1] A. Dussaux, A. V. Khvalkovskiy, P. Bortolotti, J. Grollier, V. Cros, and A. Fert. Field dependence of spin-transfer-induced vortex dynamics in the nonlinear regime. *Physical Review B*, 86(1):014402, July 2012.

[2] A. Chanthbouala, R. Matsumoto, J. Grollier, V. Cros, A. Anane, A. Fert, A. V. Khvalkovskiy, K. A. Zvezdin, K. Nishimura, Y. Nagamine, H. Maehara, K. Tsunekawa, A. Fukushima, and S. Yuasa. Vertical-current-induced domain-wall motion in MgO-based magnetic tunnel junctions with low current densities. *Nature Physics*, 7(8):626–630, April 2011.

[3] A. S. Jenkins, E. Grimaldi, P. Bortolotti, R. Lebrun, H. Kubota, K. Yakushiji, A. Fukushima, G. de Loubens, O. Klein, S. Yuasa, and V. Cros. Controlling the chirality and polarity of vortices in magnetic tunnel junctions. *Applied Physics Letters*, 105(17):172403, October 2014.

[4] A. Dussaux, A. V. Khvalkovskiy, J. Grollier, V. Cros, A. Fukushima, M. Konoto, H. Kubota, K. Yakushiji, S. Yuasa, K. Ando, and A. Fert. Phase locking of vortex based spin transfer oscillators to a microwave current. *Applied Physics Letters*, 98(13):132506, 2011.

[5] R. Lebrun, A. S. Jenkins, A. Dussaux, N. Locatelli, S. Tsunegi, E. Grimaldi, H. Kubota, P. Bortolotti, K. Yakushiji, J. Grollier, A. Fukushima, S. Yuasa, and V. Cros. Understanding of phase noise squeezing under fractional synchronization of non-linear spin transfer vortex oscillator. *arXiv:1502.03485*, February 2015.

[6] K. Yu. Guslienko, B. A. Ivanov, V. Novosad, Y. Otani, H. Shima, and K. Fukamichi. Eigenfrequencies of vortex state excitations in magnetic submicron-size disks. *Journal of Applied Physics*, 91(10):8037, 2002.